Spectrochimica Acta Part A 77 (2010) 199–206

Contents lists available at ScienceDirect

Spectrochimica Acta Part A: Molecular and Biomolecular Spectroscopy

journal homepage: www.elsevier.com/locate/saa

Spectral characterization and antimicrobial activity of 2-(5-chloro/nitro-1*H*-benzimidazol-2-yl)-4-bromo/nitro-phenols and their zinc(II) complexes

Aydin Tavman[a,*], Ismail Boz[b], A. Seher Birteksöz[c]

[a] *Istanbul University, Faculty of Engineering, Department of Chemistry, 34320, Avcılar, Istanbul, Turkey*
[b] *Istanbul University, Faculty of Engineering, Department of Chemical Engineering, 34320, Avcılar, Istanbul, Turkey*
[c] *Istanbul University, Faculty of Pharmacy, Department of Pharmaceutical Microbiology, 34452, Beyazit, Istanbul, Turkey*

ARTICLE INFO

Article history:
Received 9 October 2009
Received in revised form 4 May 2010
Accepted 15 May 2010

Keywords:
Chloro/nitro-benzimidazole
Bromo/nitro-phenols
Zinc(II) complexes
Antimicrobial activity

ABSTRACT

2-(5-Chloro/nitro-1*H*-benzimidazol-2-yl)-4-bromo/nitro-phenols (HL_x; $x = 1–4$) and their complexes with zinc(II)nitrate have been synthesized and characterized. In the tetrahedral mononuclear complexes, the ligands are bidentate, via the imine nitrogen and the phenolate oxygen atoms. The structures of the complexes were confirmed on the basis of elemental analysis, molar conductivity, TGA, FT-IR, NMR, mass and UV–vis spectroscopy. The optimized geometry of the complexes was derived from theoretical calculation in DGauss/DFT level on CACHE program. From theoretical calculations it was found that bromo derivatives of the ligands (HL_1 and HL_3) have higher stability than the other ligands and similarly, their Zn(II) complexes have higher stability than the other complexes. The antimicrobial activities of the compounds were evaluated using the disk diffusion method against six bacteria and *Candida albicans*. All of the complexes exhibited selective antibacterial activity on *Staphylococcus epidermidis*. HL_3 and $[Zn(L_1)_2]\cdot H_2O$ are more active than Ciprofloxazin and, $[Zn(L_2)_2]$ has antibacterial activity as potent as Ciprofloxazin against *S. epidermidis*.

1. Introduction

Benzimidazole derivatives display a wide range of biological and pharmacological activity. For instance, vitamin B_{12} has 5,6-dimethylbenzimidazole moiety as coordinated to the cobalt atom [1,2]. On the other hand, various drugs and pharmaceutical compositions contain benzimidazole derivatives. The perhaps most important one is an antisecretory agent, omeprazole [5-methoxy-2-(4-methoxy-3,5-dimethylpyridin-2-yl-methylsulfinyl)-1*H*-benzimidazole] [3]. The other important benzimidazol derivatives, which are used as drugs, are thiabendazole [4,5], albendazole, mebendazole, flubendazole [6,7] astemizole [8] and fenbendazole [9]. In our previous studies, we found that various benzimidazolyl-phenol derivatives showed antimicrobial activity against several microorganisms [10–15].

Zinc is an essential element and exists in multitudes of enzymes and serves many vital biological roles in the biochemical systems. It plays an active catalytic role and acts in regulatory or structural roles. The unique feature of all structurally active mononuclear zinc sites is the presence of a water molecule in the structure, which can be activated by ionization, by polarization, or be poised for displacement by a substrate. The most known enzymes containing zinc ion are carbonic anhydrase, carboxypeptidase, alcohol dehydrogenase, thermolysin and β-lactamase. Zn(II) ion plays a role in binding the water molecules and hydroxyl ions, and catalyzes the hydration/dehydration mechanisms in the enzymes [16].

Various biological activities of many Zn(II) complexes were investigated. For example, Zn(II) complexes of 1,2-bis-[(5-Cl/NO_2)-2-1*H*-benzimidazolyl]-1,2-ethanediols were effective on *Staphylococcus aureus* and *Staphylococcus epidermidis* [17]. Zn(II) complexes of some 2-pyridinyl-1*H*-benzimidazoles showed selective antimicrobial effect against *S. aureus* and *S. flexneri* although the ligands themselves had no effect [18]. Antibacterial activity of 1-benzylbenzimidazole derivatives and their Zn(II) complexes was evaluated. It was found that all the tested compounds were more active against Gram-positive bacteria as compared to activities against Gram-negative bacteria [19]. Antimicrobial activity of Zn(II), Ni(II), Cu(II) and Co(II) complexes of thiabendazole against *Escherichia coli*, *B. subtilis* and *A. flavues* organisms was estimated. The relationship between the enzymatic production of reactive oxygen species (ROS) and antimicrobial activity of the complexes was examined, and a good correlation between two factors was found [5].

* Corresponding author. Tel.: +90 212 473 70 70; fax: +90 212 473 70 79.
E-mail address: atavman@istanbul.edu.tr (A. Tavman).

1386-1425/$ – see front matter © 2010 Elsevier B.V. All rights reserved.
doi:10.1016/j.saa.2010.05.008

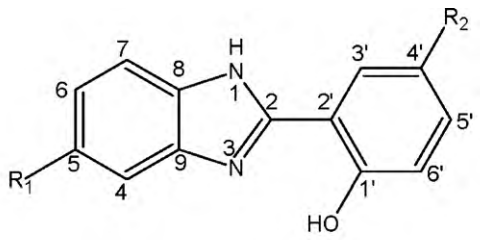

The structure of the ligands:

R_1=Cl, R_2=Br, HL_1 R_1=Cl, R_2=NO_2, HL_2

R_1=NO_2, R_2=Br, HL_3 R_1=NO_2, R_2=NO_2, HL_4.

Fig. 1. The structure of the ligands: R_1 = Cl, R_2 = Br, HL_1; R_1 = Cl, R_2 = NO_2, HL_2; R_1 = NO_2, R_2 = Br, HL_3; R_1 = NO_2, R_2 = NO_2, HL_4.

Antibacterial activity of pyridine-3,5-bis(benzimidazole-2-yl) and its Zn(II) complex was investigated and a selective inhibition property was observed for the tested strains [20]. Lukevics et al. studied antitumor activity of trimethylsilylpropyl substituted benzimidazoles and their $ZnCl_2$, $CuCl_2$, $CoCl_2$, $PdCl_2$ and $AgNO_3$ complexes and they found that cytotoxicity of benzimidazole metal complexes strongly depended on the nature of metal [21]. Antimicrobial activity of Zn(II), Fe(III), Cd(II) and Hg(II) complexes with 2,6-bis(benzimidazol-2-yl)pyridine was also studied and it was found that $M(L)Cl_2$ (M = Zn, Hg) complexes were exceptionally effective in comparison to most of the reference antibiotics on bacteria and fungi [22]. Antibacterial and antifungal activity of Zn(II), Co(II), Ni(II), Cd(II) complexes of pyridazinone was evaluated and found that the complexes had considerable antimicrobial activity [23].

In this work, 2-(5-chloro/nitro-1*H*-benzimidazol-2-yl)-4-bromo/nitro-phenols ligands (Fig. 1) and their zinc(II) nitrate complexes were studied. This study is a part of a continuing project on benzimidazoles. Our aim is to characterize and study the effect of electron withdrawing substituent's on benzimidazolyl-phenol derivatives and their Zn(II) complexes. We also aim to investigate antimicrobial activity of the ligands and the complexes against six bacteria and *Candida albicans* as yeast. Herein, we also discuss the differences of metal ion complexes with the free ligands in their structural–biological activity relationship.

2. Experimental

2.1. Chemistry and apparatus

All chemicals and solvents are of reagent grade and were used without further purification.

Elemental analysis data were obtained with a Thermo Finnigan Flash EA 1112 analyzer. Decomposition points were determined using an Electro thermal melting-point apparatus. Molar conductivity of the complexes was measured on a WTW Cond315i conductivity meter in DMSO at 25 °C. ^{1}H and ^{13}C NMR spectra were run on a Varian Unity Inova 500 NMR spectrometer. The residual DMSO-d_6 signal was also used as an internal reference. FT-IR spectra were recorded in KBr disks on a Nicolet 380 FT-IR spectrometer. UV–vis spectra was performed on a Perkin Elmer Lambda 25 UV/visible spectrometer. The Electron Spray Ionization-Mass Spectroscopy (ESI-MS) analyses were carried out in positive ion modes using a Thermo Finnigan LCQ Advantage MAX LC/MS/MS. Thermo gravimetric (TG) studies were made on a TG-60WS Shimadzu, with a heating rate of 10 °C/min under flowing air at the rate of 50 ml/min.

2.2. Synthesis of the ligands: general procedure

The ligands were prepared according to the literature procedures [24,25]. For instance, 2-(5-chloro-1*H*-benzimidazol-2-yl)-4-nitro-phenol (HL_2) was obtained by reaction of 2-hydroxy-5-nitrobenzaldehyde (1.67 g, 10 mmol) with an equivalent amount of $NaHSO_3$ (1.04 g, 10 mmol) at room temperature in 25 ml ethanol for 4–5 h. The mixture was treated with 4-chloro-1,2-phenylenediamine (1.42 g, 10 mmol) in 15 ml dimethylformamide and gently refluxed for 2 h. The reaction mixture was then poured into 500 ml icy water, filtered and crystallized from ethanol. This method was selected because of its ease, high yields and shorter synthesis time. This intermediate compound (namely, bisulfite compound of the aldehyde) was utilized to catalyze the benzimidazole synthesis since 1,2-phenylenediamines and aldehydes do not give cyclization reaction by themselves under mild conditions and possibly might lead to Schiff bases.

2.3. Synthesis of the complexes

$[Zn(L_4)_2]\cdot 2H_2O$: HL_4 ligand (150 mg, 0.5 mmol) was suspended in 10 ml ethyl acetate. $Zn(NO_3)_2\cdot 6H_2O$ (190 mg, >0.5 mmol) solution in 15 ml ethyl acetate was added to the ligand solution. After 2 h of reflux, the dark green precipitate was filtered, washed with 5 ml of ethyl acetate and dried at 70 °C.

The other complexes were prepared in a similar manner to complex $[Zn(L_4)_2]\cdot 2H_2O$ and the results are presented in Table 1.

2.4. Determination of antimicrobial activity

Antimicrobial activity against *S. aureus* ATCC 6538, *S. epidermidis* ATCC 12228, *E. coli* ATCC 8739, *Klebsiella pneumoniae* ATCC 4352, *Pseudomonas aeruginosa* ATCC 27853, *Proteus mirabilis* ATCC 14153 and *Candida albicans* ATCC 10231 were determined by the microbroth dilutions technique strictly following the recommendations of National Committee for Clinical Laboratory Standards (NCCLS) [26,27]. Mueller-Hinton broth for bacteria, RPMI-1640 medium buffered to pH 7.0 with MOPS for yeast strain was used as the test medium. Serial twofold dilutions ranging from 5000 μg/ml to 4.9 μg/ml were prepared in medium. The inoculum was prepared using a 4–6 h broth culture of each bacteria and 24 culture of yeast strains adjusted to a turbidity equivalent to a 0.5 McFarland standard, diluted in broth media to give a final concentration of 5×10^5 cfu/ml for bacteria and 0.5×10^3 to 2.5×10^3 cfu/ml for yeast in the test tray. The trays were covered and placed in plastic bags to prevent evaporation. The trays containing Mueller-Hinton broth were incubated at 35 °C for 18–20 h and the trays containing RPMI-1640 medium were incubated at 35 °C for 46–50 h. The minimum inhibitory concentrations (MIC) were defined as the lowest concentration of compound giving complete inhibition of visible growth. Antimicrobial effects of the solvents were investigated against test microorganisms.

2.5. Theoretical calculation

The structure of the complexes (shown in Fig. 7) was refined by performing a geometry optimization routine in DGauss/DFT (density functional theory) available on CACHE work system pro version 6.1.10 package program. The B88-PW91 with the DZVP basis set correlation functional of the generalized gradient approximation (GGA) was used in calculations. The lowest energy values obtained by using the DFT calculations are: HL_1 (−3696), HL_2 (−1344), HL_3 (−3441), HL_4 (−1073), $Zn(L_1)_2$ (−9205), $Zn(L_2)_2$ (−4468), $Zn(L_3)_2$ (−8697) and $Zn(L_4)_2$ (−3958); values inside parameters were in a.u.

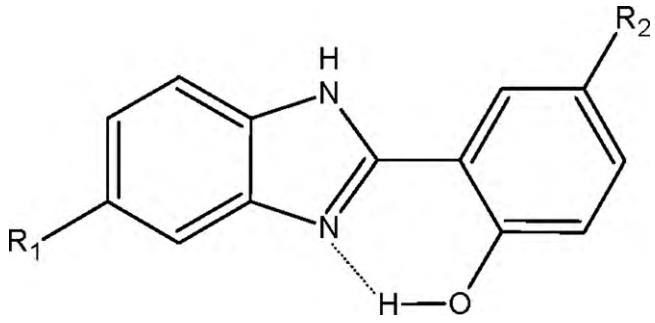

Fig. 2. The intramolecular hydrogen bonding in the ligands.

3. Results and discussions

The analytical and physical properties of the ligands and the complexes are summarized in Table 1.

The high decomposition point of the ligands (between 277 and 328 °C) and especially of the chelate complexes (>350 °C) is an evidence of that these compounds have high thermal stability. Molar conductivity of the complexes in DMSO showed that all complexes are non-electrolytes (Table 1).

3.1. IR spectra

FT-IR spectral data of the ligands and the complexes are given in Table 2. The characteristic ν(O–H) and ν(N–H) vibration frequencies of the ligands exhibit only a single strong band at *ca.* 3300 cm^{-1} in the IR spectra, caused by intramolecular hydrogen bonding between the phenoxyl hydrogen atom and C=N nitrogen atom (Table 2 and Fig. 2) [15,28–30].

Appearance of a medium broad bands between 3444 and 3523 cm^{-1} in the Zn(II) complexes of HL_1, HL_3 and HL_4 ligands strongly support the idea of the presence of water molecule(s). The N–H stretching vibrations of the ligands are observed at wavenumbers between 3227 and 3373 cm^{-1} in the complexes, suggesting that the amine proton remained attached at the N-1 (NH) position (Fig. 1).

The characteristic ν(C–H) and δ(C–H) modes of aromatic rings in the ligands and the complexes are observed at 3125–3072 and 850–720 cm^{-1} (Table 2 and Fig. 3) regions, respectively [15]. The benzene C=C and the imidazole C=N stretching frequencies are expected to appear at between 1630 and 1590 cm^{-1} with their own characteristics for the ligands and the complexes in the IR spectra

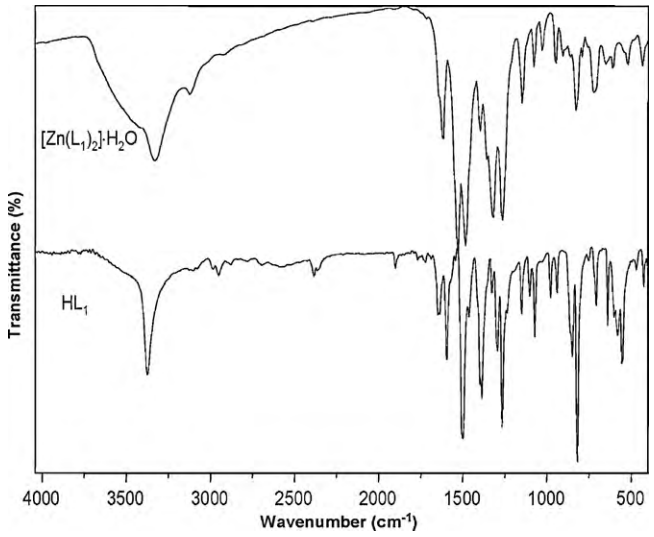

Fig. 3. FT-IR spectra of HL_1 and $[Zn(L_1)_2]\cdot H_2O$ in the mid-IR region.

[31]. Slight but specific differences between spectra of the free ligands and the complexes in this region lead to the conclusion of the formation of new complexes.

In the IR spectra of HL_2, HL_3, HL_4 ligands and their complexes, the strong or medium bands near 1500 cm^{-1} (1532–1483 cm^{-1}) and at the 1377–1305 cm^{-1} range are assigned to the symmetric and asymmetric $\nu(NO_2)$, respectively [31].

The C–Br stretching vibration is seen at 550, 515, 554 and 541 cm^{-1} as medium bands for HL_1, $Zn(L_1)_2$, HL_3, $Zn(L_3)_2$, respectively [32]. The C–Cl stretching vibration is observed at 634, 608, 649 and 641 cm^{-1} as medium or weak bands for HL_1, $Zn(L_1)_2$, HL_2, $Zn(L_2)_2$, respectively [33].

3.2. UV–vis spectra

The UV–vis spectral data are presented in Table 2. The UV–vis spectra of the ligands and the complexes in methanol showed three to five absorption bands. The lower wavelength bands (200–300 nm) correspond to $\pi \rightarrow \pi^*$ transition of the aromatic rings. The bands between 300 and 350 nm are due to $n \rightarrow \pi^*$ transitions. The visible region (>350 nm) bands in the Zn(II) complexes are due to L → Zn (oxygen → zinc) charge transfer (reason of the darker color of the complexes than the ligands) [34–36].

Table 1
The analytical and physical properties of the ligands and the complexes.

Compound	Elemental analysis Found (Calcd) (%)			Yield (%)	Dec. (°C)	Λ[a]	Color
	C	H	N				
HL_1 $C_{13}H_8BrClN_2O$	48.4 (48.2)	2.8 (2.5)	8.6 (8.7)	64	309	–	Dirty white
HL_2 $C_{13}H_8ClN_3O_3$	54.2 (53.9)	3.1 (2.8)	14.4 (14.5)	63	328	–	Yellow
HL_3 $C_{13}H_8BrN_3O_3$	46.4 (46.7)	2.6 (2.4)	12.8 (12.6)	58	277	–	Dark yellow
HL_4 $C_{13}H_8N_4O_5$	52.3 (52.0)	3.1 (2.7)	18.4 (18.7)	70	318	–	Dark yellow
$[Zn(L_1)_2]\cdot H_2O$ $C_{26}H_{16}Br_2Cl_2N_4O_3Zn$	42.5 (42.9)	2.0 (2.2)	7.4 (7.7)	74	>350	8	Dark yellow
$[Zn(L_2)_2]$ $C_{26}H_{14}Cl_2N_6O_6Zn$	48.6 (48.6)	2.7 (2.2)	12.6 (13.1)	80	>350	13	Dark yellow
$[Zn(L_3)_2]\cdot 2H_2O$ $C_{26}H_{18}Br_2N_6O_8Zn$	41.1 (40.7)	2.5 (2.4)	11.4 (10.9)	73	>350	15	Light brown
$[Zn(L_4)_2]\cdot 2H_2O$ $C_{26}H_{18}N_8O_{12}Zn$	44.2 (44.6)	2.9 (2.6)	16.5 (16.0)	63	>350	21	Dark green

[a] Λ, molar conductivity in DMSO, Ω^{-1} cm^2 mol^{-1} (25 °C). Dec., decomposition.

Table 2
FT-IR and UV–vis spectral data of the ligands and the complexes.

Compound	Frequency (cm^{-1}), KBr pellets	Wavelength (nm), in MeOH
HL_1	3340s, 3072m, 2921m, 1632m, 1623m, 1580m, 1485s, 1377s, 1284m, 1255s, 1140m, 1062m, 843m, 812s, 634m, 577m, 550m, 424m	226, 246sh, 292, 300, 327, 341
$[Zn(L_1)_2]\cdot H_2O$	3451m,br, 3296m, 3093m,br, 1625m, 1598m, 1515s, 1471s, 1351m, 1308m, 1255m, 1069m, 824m, 723m, 608m, 515m, 429m	229sh, 254, 262, 268, 326, 344, 366br, 382, 437br
HL_2	3263s, 3097w, 1630m, 1608m, 1587s, 1488m, 1396m, 1338s, 1317s, 1296s, 1133s, 1062m, 937m, 807m, 748m, 649m, 573m	211, 228, 297, 320, 335, 356sh, 402br
$[Zn(L_2)_2]$	3279s, 3112m, 1624m, 1598m, 1561m, 1489s, 1346s, 1314s, 1135s, 1062m, 838m, 805m, 752m, 645m, 508w	223, 269, 297, 320, 334, 412br, 477br
HL_3	3327m,br, 3085m, 1630m, 1597m, 1583m, 1518s, 1483s, 1339s, 1322s, 1249s, 1065m, 970m, 817m, 737m, 633m, 554m, 468w	214, 230, 263 269, 349
$[Zn(L_3)_2]\cdot 2H_2O$	3460m,br, 3373m,br, 3104m, 1631m, 1604m, 1527m, 1515m, 1474m, 1345m, 1248m, 1144m, 1060m, 819m, 738m, 624m, 541m, 465w	216, 226, 264 351, 498
HL_4	3264m, 3100m, 1659m, 1631m, 1612m, 1592m, 1518m, 1483m, 1342s, 1329s, 1299s, 1129m, 891m, 812m, 736m, 643m, 569w, 468w	228, 262, 269, 342, 413br
$[Zn(L_4)_2]\cdot 2H_2O$	3523m,br, 3227m,br, 3123m, 1626m, 1610m, 1563m, 1532m, 1488s, 1350s, 1305s, 1135s, 1085m, 900m, 820m, 732m, 628m, 473w	230, 268, 299br, 337, 486br, 538br

3.3. NMR spectra

^{1}H NMR spectral data and their assignments are presented in Table 3. ^{1}H NMR spectra of HL_2 and $[Zn(L_2)_2]$ are presented in Fig. 4. The ^{1}H NMR spectra of HL_2 and HL_4 ligands exhibit only a single broad band for the OH and the amine NH protons (13.81 and 13.61 ppm for HL_2 and HL_4, respectively). This combination results from strong intramolecular hydrogen bonding between the amine nitrogen with double bond and phenolic hydrogen atoms (Fig. 2) [33,37]. In the HL_3 spectra two broad singlets are observed for these protons. The NH and OH protons could not be detected in HL_1 spectra (Table 3).

In the literature, ^{1}H NMR spectrum of benzimidazole was reported firstly by Black and Heffernan (in CD_3OD) [38]. They reported that H4 (or H7) protons appeared at 7.61 ppm and H5 (or H6) protons at 7.24 ppm. On the other hand, Claramunt et al. studied the tautomerism of omeprazole in THF-d_8 by means of NMR spectra [39]. They reported that the signals of H4 and H7 protons were observed at 7.26 and 7.41 ppm, respectively. H6 proton appeared at 6.91 ppm. Similarly, the NMR spectral studies of some 2-(2-hydroxyphenyl)-1*H*-benzimidazole derivatives were also reported [25,28,40].

It is observed that benzimidazole ring protons of HL_1 and HL_2 (having chloro substituent 5-position on the benzimidazole ring) appear below 8.0 ppm (Fig. 4). Namely, 8.31 and 9.06 ppm signals must belong to the H3′ proton in the spectra of HL_1 and HL_2, respectively. The ppm values of H4 protons of HL_1, HL_2, $[Zn(L_1)_2]\cdot H_2O$ and $[Zn(L_2)_2]$ are 7.73, 7.76, 7.91, 7.99, respectively (Fig. 4). However, the protons neighboring to the nitro group (HL_2, HL_3 and HL_4) are observed at above 8.0 ppm. HL_3 and HL_4 have a nitro group at the 5-position on the benzimidazole ring. The chemical shift values of H4 protons of HL_3, HL_4, $[Zn(L_3)_2]\cdot 2H_2O$ and $[Zn(L_4)_2]\cdot 2H_2O$ are 8.51, 8.60, 8.94, 9.00 ppm, respectively. It is known that the nitro group on aromatic ring moves the resonance of the *ortho* protons downfield by approximately +0.95 ppm, while bromine and chlorine atoms move them approximately +0.2 and 0.0 ppm, respectively [41].

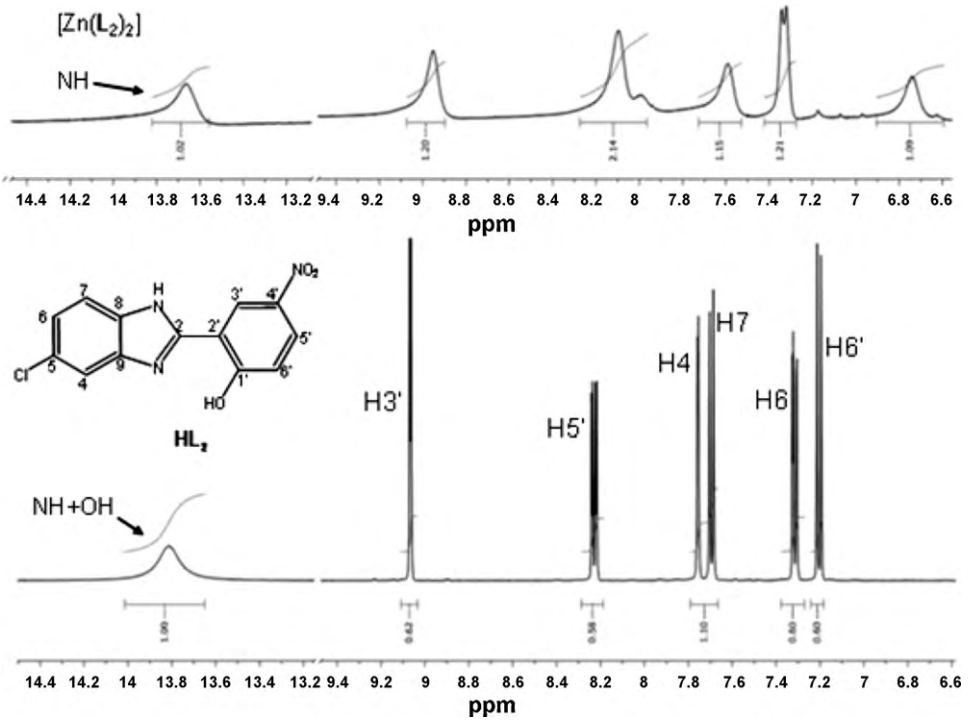

Fig. 4. ^{1}H NMR spectra of HL_2 and $[Zn(L_2)_2]$.

Table 3
^{1}H NMR spectral data (the chemical shift values, δ_H, ppm, with coupling constants, J, Hz, in DMSO-d_6).

Compound	The benzimidazole protons				The phenolic protons			
	H4	H6	H7	NH	H3′	H5′	H6′	OH
HL_1	7.73 d J = 1.9	7.33 d-d J = 8.8, 1.9	7.69 d J = 8.8	–[a]	8.31 d J = 2.4	7.53 d-d J = 8.8, 2.4	7.07 d J = 8.8	–[a]
$[Zn(L_1)_2]\cdot H_2O$	7.91 d J = 2.6	8.07 d-d J = 9.3, 2.7	7.54 s,br	13.53 s,br	8.26 s	7.28 s,br	6.68 d,br J = 9.1	–
HL_2	7.76 d J = 2.0	7.31 d-d J = 2.1, 8.8	7.69 d J = 8.7	13.81 s,br	9.06 d J = 3.1	8.23 d-d J = 9.1, 3.1	7.20 d J = 9.3	13.81 s,br
$[Zn(L_2)_2]$	7.99 s,br	8.09 s,br	7.32 d,br J = 10.4	13.65 s,br	8.97 s,br	7.69 s,br	6.73 s,br	–
HL_3	8.51 s,br	8.14 d-d J = 8.9, 1.5	7.78 d J = 8.8	13.41 s,br	8.29 d J = 2.2	7.55 d-d J = 8.8, 2.4	7.04 d J = 8.9	12.37 s,br
$[Zn(L_3)_2]\cdot 2H_2O$	8.94 s	7.82 s,br	7.71 s,br	13.44 s,br	8.15 d,br J = 2.4	7.38 s,br	6.83 s,br	–
HL_4	8.60 s,br	8.20 d-d J = 1.8, 8.7	7.88 d J = 8.7	13.61 s,br	9.13 d J = 2.7	8.30 d-d J = 2.7, 8.9	7.28 d J = 8.9	13.61 s,br
$[Zn(L_4)_2]\cdot 2H_2O$	9.00 s,br	8.14 s,br	7.81 d,br J = 6.8	–[a]	9.00 s,br	8.19 d-d J = 8.8, 2.0	6.96 s,br	–

[a] Not detected.

Indeed, it is observed that the nitro groups move the resonance of the *ortho* protons (H4, H6, H3′ and H5′) downfield (above 8.0 ppm) in the ^{1}H NMR spectra of HL_4 and its Zn(II) complex.

It is observed that the doublets and doublets of doublets at the NMR spectra of the ligands which belong to the protons of the benzimidazole benzene and phenol rings, changed to broad doublets on complexation. It is interesting to note that H3′ and H4 protons in $[Zn(L_4)_2]\cdot 2H_2O$ complex show a broad singlet at almost the same position, 9 ppm.

^{13}C NMR spectral data are given in Table 4. In the ^{13}C NMR spectra of the ligands and the complexes the signals at the highest ppm values (over 150 ppm), e.g. 157.6 and 150.6 ppm for HL_1, belong to C1′, bonded to the OH oxygen, and imidazole C=N (C2) carbon atoms, respectively [39]. NMR signals belonging to C8, C9 and also the carbon atoms that bonded to the nitro group appear at the 140–150 ppm region. The other signals belong to the benzimidazole benzene and phenol rings carbon atoms (Table 4). Good quality ^{13}C NMR spectra for $[Zn(L_2)_2]$ and $[Zn(L_4)_2]\cdot 2H_2O$ complexes could not be recorded because of their low solubility characters in DMSO-d_6 and in the other strong solvents such as methanol and DMF, too.

3.4. Mass spectra

The ESI-MS spectral data of the complexes are given in Table 5 as molecular ions with the relative abundance. The assignments of the some intense ions are given in Table 5, also. Molecular ions of the complexes are observed in their ESI-MS spectra. The ions for $Zn(L_3)_2$ and $Zn(L_4)_2$, $[M-2H_2O]^+$, are present at m/z values of 729.6 and 663.2, respectively (Fig. 5). Also, the peaks of the ligands are easily determined in the mass spectra of the complexes (the ligands are shown as L in Table 5).

The higher m/z values than the molecular ions may be due to condensation products of lower mass ions. Some of the higher m/z values according to the molecular ions can be interpreted as forming of the polymeric structures under ESI-MS conditions.

3.5. Thermogravimetric analyses

The major features of the thermal analysis of the complexes are summarized in Table 6. TGA curves of $[Zn(L_1)_2]\cdot H_2O$, $[Zn(L_2)_2]$ and $[Zn(L_4)_2]\cdot 2H_2O$ complexes are shown in Fig. 6.

In the TG analysis of $[Zn(L_2)_2]$, there is no comparatively significant weight loss until 300 °C. At about 300 °C, a weight loss of 3.1% is observed (Fig. 6). This finding alone is explained as a proof

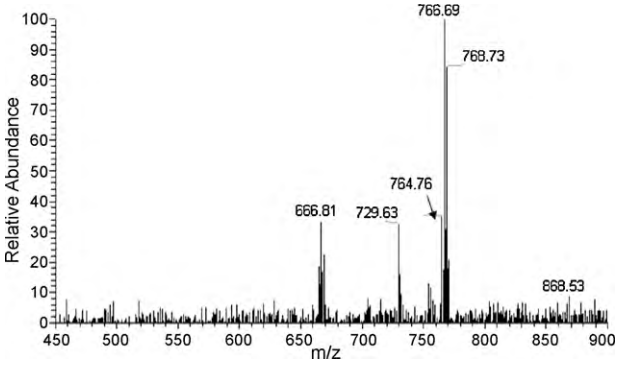

Fig. 5. ESI-MS spectra of $[Zn(L_3)_2]\cdot 2H_2O$.

of non-existence of coordinated and uncoordinated water molecule [42–45] and, it is in line with the ESI-MS data and elemental analysis of $[Zn(L_2)_2]$ complex.

TGA curves showed that decomposing of the complexes start above 350 °C except $[Zn(L_4)_2]\cdot 2H_2O$. $[Zn(L_4)_2]\cdot 2H_2O$ starts to decompose above 200 °C. On the other hand, it is observed that a considerable weight loss occurred in this complex. This complex contains two nitro groups and, it is assumed that weight loss is due to the elimination of two nitro groups above 200 °C. This result is in

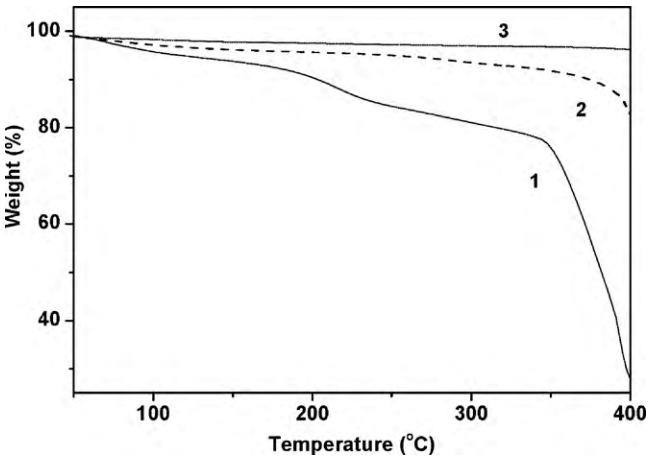

Fig. 6. TGA curves of $[Zn(L_4)_2]\cdot 2H_2O$ (1), $[Zn(L_1)_2]\cdot H_2O$ (2) and $[Zn(L_2)_2]$ (3) complexes.

Table 4
^{13}C NMR spectral data (in DMSO-d_6).

Compound	Chemical shifts (δ_C, ppm)
HL_1	157.6, 150.6, 135.8, 130.2, 128.8, 124.7, 116.7, 115.1, 114.3, 111.1
$[Zn(L_1)_2]\cdot H_2O$	161.0, 152.6, 144.8, 134.8, 129.8, 128.2, 126.6, 119.8, 100.7
HL_2	164.1, 151.5, 140.4, 128.4, 127.9, 124.3, 124.0, 118.9, 113.6
$[Zn(L_2)_2]$	153.2, 128.1, 128.7, 126.2, 117.1
HL_3	160.0, 157.5, 143.8, 135.6, 134.6, 132.2, 130.3, 129.4, 120.2, 119.7, 115.4, 111.2, 110.9
$[Zn(L_3)_2]\cdot 2H_2O$	157.4, 153.9, 143.9, 141.1, 137.1, 136.0, 130.3, 120.1, 119.4, 115.4, 114.6, 112.2. 111.2
HL_4	163.7, 154.0, 144.0, 140.5, 128.4, 125.0, 119.4, 118.9, 114.2
$[Zn(L_4)_2]\cdot 2H_2O$	143.8, 132.3, 129.4, 128.5, 119.9, 119.6, 110.0

Table 5
ESI-MS spectral data of the complexes.

Compound and MW (g/mol)	Molecular ions (m/z) with relative abundance (%) and assignments[a]
$[Zn(L_1)_2]\cdot H_2O$ 728.5	732.5 (23.6, $[MH_4]^+$), 424.6 (15.3, $[L+Zn+2H_2O]^+$), 387.8 (12.5, $[L+Zn]^+$), 368.3 (25.9, $[(L+Zn)-OH-3H]^+$), 322.9 (100, L)
$[Zn(L_2)_2]$ 642.7	641.3 (26.9, $[M-1]^+$), 550.0 (19.5, $[M-2NO_2]^+$), 352.1 (12.3, $[M-L-1]^+$), 289.6 (100, L)
$[Zn(L_3)_2]\cdot 2H_2O$ 767.6	766.7 (100, $[M-H]^+$), 768.7 (83.5, $[M+1]^+$), 729.6 (33.2, $[M-2H-2H_2O]^+$), 666.8 (34.9, 2L), 434.5 (10.5, $[L+Zn+2H_2O]^+$), 396.9 (27.5, $[L+Zn]^+$), 334.2 (25.5, L)
$[Zn(L_4)_2]\cdot 2H_2O$ 699.9	697.4 (9.3, $[M-2H]^+$), 682.1 (7.0, $[M-H_2O]^+$), 663.2 (100, $[M-2H_2O]^+$), 597.8 (7.2, 2L), 410.2 (50.5), 298.9 (32.5, L)

[a] The ligands are shown as L.

Table 6
TGA data of the complexes (thermal decompositions).

Complex	Temperature (°C)						
	110	150	200	250	300	350	400
	Weight loss (%)						
$[Zn(L_1)_2]\cdot H_2O$	3.4	3.8	4.2	5.5	7.6	9.8	16.7
$[Zn(L_2)_2]$	0.8	1.2	1.9	2.3	3.1	3.9	4.6
$[Zn(L_3)_2]\cdot 2H_2O$	5.2	7.1	7.3	8.4	11.3	15.4	51.0
$[Zn(L_4)_2]\cdot 2H_2O$	4.5	6.9	10.8	15.8	19.1	25.2	73.2

agreement with the theoretical calculations. According to the theoretical calculations $[Zn(L_4)_2]\cdot 2H_2O$ has the lowest stability among the complexes (see Section 3.7).

In the TG analysis of $[Zn(L_4)_2]\cdot 2H_2O$ complex, a weight loss is observed for 4.5% ratio at *ca.* 100 °C (Fig. 6). This figure corresponds to two moles of uncoordinated lattice water molecules [46,47]. Theoretical weight loss for two moles of water is 5.1%. $[Zn(L_1)_2]\cdot H_2O$ and $[Zn(L_3)_2]\cdot 2H_2O$ complexes have similar TG curves to that of $[Zn(L_4)_2]\cdot 2H_2O$. TGA curves of the complexes are consistent with the theoretical weight losses for their water contents.

3.6. Microbial activity

The results concerning *in vitro* antimicrobial activity of the ligands and the complexes together with MIC values of compared antibiotic and antifungal reagents are presented in Table 7.

Actually six bacteria and only one fungus have been studied in antimicrobial activity tests. The antimicrobial activity results show that all of the complexes have selective antibacterial effect on *S. epidermidis*. It is unambiguous that HL_3, $HL_3\cdot HCl$, $[Zn(L_1)_2]\cdot H_2O$ and $[Zn(L_3)_2]\cdot 2H_2O$ have considerable antibacte-

Table 7
In vitro antimicrobial activity of the compounds (MIC, μg/ml).

Compound	Microorganisms						
	Sa[a]	*Se*[a]	*Ec*[b]	*Kp*[b]	*Pa*[b]	*Pm*[b]	*Ca*
HL_1	–	–	–	–	–	–	–
$HL_1\cdot HCl$	–	–	–	–	–	–	–
HL_2	312	–	–	–	–	–	–
$HL_2\cdot HCl$	–	–	–	–	–	–	–
HL_3	2.4	19.5	–	–	–	–	–
$HL_3\cdot HCl$	2.4	2.4	–	–	–	–	–
HL_4	78	–	–	–	–	–	–
$HL_4\cdot HCl$	–	–	–	–	–	–	–
$[Zn(L_1)_2]\cdot H_2O$	2.4	2.4	–	–	–	–	–
$[Zn(L_2)_2]$	–	156	–	–	–	–	–
$[Zn(L_3)_2]\cdot 2H_2O$	19.5	156	–	–	–	–	–
$[Zn(L_4)_2]\cdot 2H_2O$	–	156	–	–	–	–	–
$Zn(NO_3)_2\cdot 6H_2O$	–	–	–	–	–	–	–
Ciprofloxazin	0.125	156	0.0625	0.0625	2.00	0.0312	–
Fluconazole	–	–	–	–	–	–	1.0

Sa Staphylococcus aureus ATCC 6538; *Se Staphylococcus epidermidis* ATCC 12228; *Ec Escherichia coli* ATCC 8739; *Kp Klebsiella pneumoniae* ATCC 4352; *Pa Pseudomonas aeruginosa* ATCC 1539; *Pm Proteus mirabilis* ATCC 14153; *Ca Candida albicans* ATCC 10231.
–, antimicrobial activity was not detected.
[a] Gram(+).
[b] Gram(−).

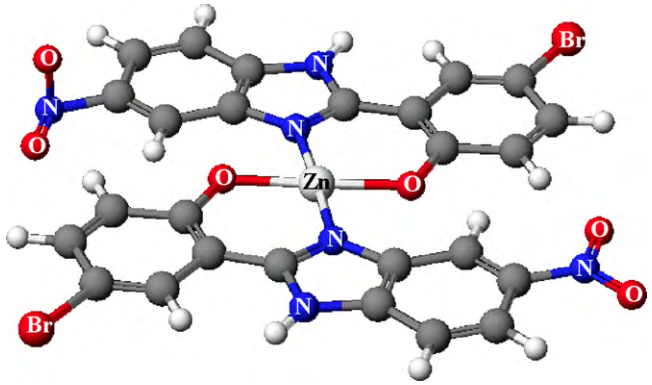

Fig. 7. Optimized structure of $Zn(L_3)_2$ complex.

rial effect on *S. aureus* and *S. epidermidis*. Also, it is seen that HL_3 and $[Zn(L_1)_2]\cdot H_2O$ are more active than Ciprofloxazin reference drug; and microbial activity of $[Zn(L_2)_2]$ complex is as potent as Ciprofloxazin against *S. epidermidis*. The antibacterial data indicate that the bromo substituted ligands and their complexes have a very strong and penetrating activity against Gram+ bacteria. For instance, $HL_3\cdot HCl$ and $[Zn(L_1)_2]\cdot H_2O$ showed superior activity (MIC = 2.4 μg/ml for both of them) against *S. epidermidis* (Gram+) than the reference Ciprofloxazin (MIC = 156 μg/ml).

Microbial activity of HL_1 and $Zn(NO_3)_2$ against the selected microorganisms in our study is found to be insignificant. On the other hand, $[Zn(L_1)_2]\cdot H_2O$ complex showed superior activity against *S. epidermidis*. The results of our study indicate that particularly HL_3 and $[Zn(L_1)_2]\cdot H_2O$ have displayed activity to generate novel metabolites due to high affinities towards various receptors. The strong antimicrobial activities of these compounds especially against *S. epidermidis* warranted further investigation on these compounds.

3.7. Theoretical calculation and stability

According to the DFT calculations, HL_1, HL_3 and their Zn(II) complexes, $[Zn(L_1)_2]\cdot H_2O$ and $[Zn(L_3)_2]\cdot 2H_2O$, have higher energy values: −3695, −3441, −9205, −8695 a.u., respectively. The total energy values of HL_2, HL_4 and their complexes are: −1344, −1073, −4468, −3958 a.u., respectively. The DFT calculations prove that the bromo derivatives have higher stability than the nitro and chloro derivatives, comparing them with each other.

It is observed that HL_1, having bromo and chloro substituents, is more stable (total energy: −3695 a.u.) than HL_3, having bromo and nitro substituents (−3441 a.u.). It can be said that the nitro substituent on the HL_3 lead to a decrease in the stability. The DFT calculations show that the stability of HL_4 ligand is the lowest among the ligands probably due to two nitro substituents on the phenol and the benzimidazole benzene rings of it. Likewise, $Zn(L_4)_2$ has the highest energy among the complexes and consequently the lowest stability: −3958 a.u. Also, this result is consistent with the TGA data of $[Zn(L_4)_2]\cdot 2H_2O$: it is observed that onset of decomposition of $[Zn(L_4)_2]\cdot 2H_2O$ is at lower temperatures than those of other complexes as explained in thermogravimetric analyses.

According to the geometry optimization of $[Zn(L)_2]$ structure with DFT calculations, Zn is located on a distorted tetrahedral center with the C=N nitrogen and hydroxy oxygen atoms of benzimidazole moiety and phenol ring, respectively (molecular symmetry: C_s). An exemplary optimized structure for $Zn(L_3)_2$ complex is given in Fig. 7.

4. Conclusions

In this work, we synthesized and characterized the chloro, bromo, nitro derivatives of 2-(1*H*-benzimidazol-2-yl)-phenols and their $Zn(NO_3)_2$ complexes. The metal:ligand ratio of the non-electrolyte complexes is 1:2. The DFT calculations proved that the bromo derivatives have higher stability than the nitro and chloro derivatives. Antimicrobial activities of the compounds were investigated towards six bacteria and a fungus. According to the antimicrobial activity results, HL_3 and $[Zn(L_1)_2]\cdot H_2O$ are more effective than Ciprofloxazin and $[Zn(L_2)_2]$ exhibited microbial activity as potent as Ciprofloxazin against *S. epidermidis*. HL_3, $HL_3\cdot HCl$, $[Zn(L_1)_2]\cdot H_2O$ and $[Zn(L_3)_2]\cdot 2H_2O$ have very strong and penetrating activity against Gram+ bacteria such as *S. aureus* and *S. epidermidis*. It is noteworthy to point out that $[Zn(L_1)_2]\cdot H_2O$ showed strong antibacterial effect while the ligand itself had no any activity. In conclusion, the structures of the mononuclear complexes were verified by FT-IR, NMR, UV–vis and ESI-MS spectroscopic methods, as well as by elemental analysis, molar conductivity and thermo gravimetric analysis. All the analytical and spectral data are consistent with the optimized structures. According to the geometry optimization, Zn(II) ion is located on a distorted tetrahedral center with the C=N nitrogen and hydroxy oxygen atoms (Fig. 7).

Acknowledgements

This work was supported by TUBITAK (The Scientific and Technological Research Council of Turkey). COST project number: TBAG-U/185 (106T086).

References

[1] R. Bonnett, Chem. Rev. 63 (1963) 573–605.
[2] N.G. Brink, K. Folkers, J. Am. Chem. Soc. 72 (1950) 4442–4443.
[3] C.S.P. Sastry, P.Y. Naidu, S.S.N. Murty, Talanta 44 (1997) 1211–1217.
[4] C. Delescluse, M.P. Piechock, N. Ledirac, R.H. Hines, R. Li, X. Gidrol, R. Rahmani, Biochem. Pharmacol. 61 (2001) 399–407.
[5] K.K. Mothilal, C. Karunakaran, A. Rajendran, R. Murugesan, J. Inorg. Biochem. 98 (2004) 322–332.
[6] E.J. Cardoso, A.F. Luna, J.P. Urizar, Acta Trop. 92 (2004) 237–244.
[7] M. Savlik, P. Polaskova, B. Szotakova, J. Lamka, L. Skalova, Res. Vet. Sci. 79 (2005) 139–147.
[8] R.G. Almeida, J.C. Florio, H.S. Spinosa, M.M. Bernardi, Neurotoxicol. Teratol. 24 (2002) 255–265.
[9] J. Gronvold, T.S. Svendsen, H.O. Kraglund, J. Bresciani, J. Monrad, Vet. Parasitol. 124 (2004) 91–99.
[10] B. Ülküseven, A. Tavman, G. Ötük, S. Birteksöz, Folia Microbiol. 47 (2002) 481–487.
[11] A. Tavman, N.M. Agh-Atabay, A. Neshat, F. Gücin, B. Dülger, D. Haciu, Transit. Met. Chem. 31 (2006) 194–200.
[12] A. Tavman, S. İkiz, A.F. Bağcıgil, Y. Özgür, S. Ak, Russ. J. Inorg. Chem. 55 (2010) 215–222.
[13] A. Tavman, S. İkiz, A.F. Bağcıgil, Y. Özgür, S. Ak, J. Serb. Chem. Soc. 74 (2009) 537–548.
[14] A. Tavman, S. İkiz, A.F. Bağcıgil, Y.N. Özgür, S. Ak, Turk. J. Chem. 33 (2009) 321–331.
[15] A. Tavman, N.M. Agh-Atabay, S. Güner, F. Gücin, B. Dülger, Transit. Met. Chem. 32 (2007) 172–179.
[16] D.E. Fenton, Biocoordination Chemistry, Oxford University Press, Oxford, 1997.
[17] A. Tavman, S. Birteksöz, G. Ötük, Folia Microbiol. 50 (2005) 473–478.
[18] A. Tavman, B. Ülküseven, S. Birteksöz, G. Ötük, Folia Microbiol. 48 (2003) 479–483.
[19] S.O. Podunavac-Kuzmanovic, D.M. Cvetkovic, J. Serb. Chem. Soc. 72 (2007) 459–466.
[20] C.-Y. Guo, Y.-Y. Wang, K.-Z. Xu, H.-L. Zhu, P. Liu, Q.-Z. Shi, S.-M. Peng, Polyhedron 27 (2008) 3529–3536.
[21] E. Lukevics, P. Arsenyan, I. Shestakova, I. Domracheva, A. Nesterova, O. Pudova, Eur. J. Med. Chem. 36 (2001) 507–515.
[22] N.M. Agh-Atabay, A. Neshat, T. Karabiyik, M. Somer, D. Haciu, B. Dülger, Eur. J. Med. Chem. 42 (2007) 205–213.
[23] M. Sönmez, I. Berber, E. Akbaş, Eur. J. Med. Chem. 41 (2006) 101–105.
[24] H.F. Ridley, G.W. Spickett, G.M. Timmis, J. Het. Chem. 2 (1965) 453–456.
[25] A. Tavman, B. Ülküseven, Main Group Met. Chem. 24 (2001) 205–210.
[26] Clinical and Laboratory Standards Institute (CLSI), Methods for Dilution Antimicrobial Susceptibility Tests for Bacteria that Grow Aerobically, Approved Standard, M7-A5, 2006, Wayne, PA, USA.

[27] Clinical and Laboratory Standards Institute (CLSI), Reference Method for Broth Dilution Antifungal Susceptibility Testing of Yeasts, Approved Standard M27-A2, 2nd ed., 2002, Wayne, PA, USA.
[28] A. Tavman, Spectrochim. Acta A63 (2006) 343–348.
[29] D. Kanamori, Y. Yamada, A. Onoda, T.A. Okamura, S. Adachi, H. Yamamoto, N. Ueyama, Inorg. Chim. Acta 358 (2005) 331–338.
[30] N. Ueyama, N. Nishikawa, Y. Yamada, T. Okamura, A. Nakamura, Inorg. Chim. Acta 283 (1998) 91–97.
[31] K. Nakamoto, Infrared and Raman Spectra of Inorganic and Coordination Compounds, Part B, 5th ed., John Wiley & Sons Inc., New York, 1997.
[32] N. Sundaraganesan, C. Meganathan, B. Anand, C. Lapouge, Spectrochim. Acta A66 (2007) 773–780.
[33] N. Sundaraganesan, B. Anand, F.-F. Jian, P. Zhao, Spectrochim. Acta A65 (2006) 826–832.
[34] D.S. Chowdhuri, A. Rana, M. Bera, E. Zangrando, S. Dalai, Polyhedron 28 (2009) 2131–2136.
[35] G.-X. Liu, K. Zhu, S. Nishihara, R.-Y. Huang, X.-M. Ren, Inorg. Chim. Acta 362 (2009) 5103–5108.
[36] S.L. Li, Y.Q. Lan, J.F. Ma, J. Yang, G.H. Wei, L.P. Zhang, Z.M. Su, Cryst. Growth Des. 8 (2008) 675–684.
[37] F.R. Prieto, J.C. Penedo, M. Mosquera, J. Chem. Soc. Faraday Trans. 94 (1998) 2775–2782.
[38] P.J. Black, M.I. Heffernan, Aust. J. Chem. 15 (1962) 862–864.
[39] R.M. Claramunt, C. Lopez, I. Alkorta, J. Elguero, R. Yang, S. Schulman, Magn. Reson. Chem. 42 (2004) 712–714.
[40] G. Navarrete-Vazquez, L. Yepez, A. Hernandez-Campos, A. Tapia, F. Hernandez-Luis, R. Cedillo, J. Gonzalez, A. Martinez-Fernandez, M. Martinez-Grueirod, R. Castillo, Bioorg. Med. Chem. 11 (2003) 4615–4622.
[41] W. Kemp, NMR in Chemistry: A Multinuclear Introduction, 2nd ed., McMillan Education Ltd., London, 1998.
[42] K.K.M. Yusuf, R. Sreekala, Thermochim. Acta 179 (1991) 313–322.
[43] A.A. Soliman, W. Linert, Thermochim. Acta 338 (1999) 67–75.
[44] P.R. Chetana, X. Siddaramaiah, P.G. Ramappa, Thermochim. Acta 425 (2005) 13–21.
[45] S.-F. Si, R.-J. Wang, Y.-D. Li, Inorg. Chem. Commun. 6 (2003) 1152–1155.
[46] B.-M. Kukovec, Z. Popovic, J. Mol. Struct. 930 (2009) 121–125.
[47] F.-Q. Wang, D.-F. Weng, X.-J. Zheng, J.-J. Zhang, H. Ma, L.-P. Jin, Inorg. Chim. Acta 360 (2007) 2029–2038.